

Atomic bond fluctuations and crossover to potential-energy-landscape-influenced regime in supercooled liquid

V. A. Levashov

Department of Physics and Astronomy, University of Tennessee, Knoxville, Tennessee 37996, USA

T. Egami

*Department of Physics and Astronomy, University of Tennessee, Knoxville, Tennessee 37996, USA;
Department of Materials Science and Engineering, University of Tennessee, Knoxville, Tennessee 37996, USA;
and Oak Ridge National Laboratory, Oak Ridge, Tennessee 37831, USA*

R. S. Aga

Materials Science and Technology Division, Oak Ridge National Laboratory, Oak Ridge, Tennessee 37831, USA

J. R. Morris

*Materials Science and Technology Division, Oak Ridge National Laboratory, Oak Ridge, Tennessee 37831-6115 USA
and Department of Materials Science and Engineering, University of Tennessee, Knoxville, Tennessee 37996-2200, USA*

(Received 16 April 2008; revised manuscript received 14 August 2008; published 17 October 2008)

The ideas related to potential-energy landscape and cooperativity of atomic rearrangements are widely discussed in the research field of glass transition. The crossover transition from high-temperature regime to potential-energy-landscape-influenced regime was extensively studied using the concept of inherent structure. However, the interpretation of this crossover behavior in terms of microscopic changes in real structures is still lacking. In this paper we present several observations on the crossover behavior on real structures. We compare fluctuations in the global properties (total number of bonds, total potential energy, pressure) versus fluctuations in the local properties (coordination number, atomic potential energy, local atomic pressure) by means of molecular dynamics simulations. We then show that the total and local fluctuations in the number of atomic bonds in the system depend on temperature differently above and below the temperature of crossover to the landscape-influenced regime. Similarly, the ratio between the global and local fluctuations in the potential energy and pressure changes in the vicinity of the crossover temperature, whereas the change is less distinct than in the case of the bond fluctuations. Our results indicate that local fluctuations become more correlated below the crossover temperature, most likely via the interaction through the dynamic shear elastic field.

DOI: [10.1103/PhysRevE.78.041202](https://doi.org/10.1103/PhysRevE.78.041202)

PACS number(s): 61.20.Ne, 61.20.Ja, 61.43.Fs

I. INTRODUCTION

The connection between structure and dynamics is a central question in the research field of glass transition [1–3]. After many years of study it is still unclear why such properties as diffusivity, viscosity, and relaxation time change by so many orders of magnitude while there are only small apparent changes in the structure. It is also not clear if there exist universal parameters that can describe these subtle changes in the structure for all classes of liquids and glasses [4–7].

In the past decades extensive numerical studies were performed on different model systems exhibiting the glass transition. These studies indicated the presence of different dynamic regimes in supercooled liquids [1,8–10]. In particular, two temperatures are often considered to separate these regimes, in addition to the glass transition temperature T_g . One is the mode-coupling temperature T_c which is above, but is rather close to T_g [11,12]. The other is the so-called crossover temperature T_A which lies significantly above T_g or T_c , but usually below the melting temperature T_m [2]. It is often assumed that “the true supercooled liquid behavior” starts below T_A [2].

Most often the presence of the crossover temperature T_A is revealed in molecular dynamics (MD) simulations by ex-

amining the inherent structure, i.e., the structure obtained by steepest decent relaxation (quenching) of the structure at a given “real” temperature. In particular, it was shown [10] that the mean potential energy of the inherent structures exhibits a nontrivial dependence on the temperature of the original “real” structure. Thus when the system is quenched from a high temperature, the energy of the inherent structure is almost temperature independent. However, as temperature is reduced below T_A , the energy of the inherent structure starts to decrease with the decreasing original temperature.

There are also several observations of crossover behavior on real structure. In particular it was observed in the temperature dependence of the β parameter in the stretched exponential fit to the intermediate self-scattering function [10,11,13], in the temperature dependence of viscosity (i.e., breakdown of Stokes-Einstein relationship) [13,14], and in deviation from the fluctuation-dissipation relation [13]. However, while these observations are important, in our view they did not yield enough insight about the relations of these phenomena to the microscopic structure of the real liquid. The interpretation of the crossover phenomenon in terms of microscopic parameters is still absent.

In this paper we present several evidences of the crossover behavior on the real, not the inherent, structure. In our

approach we use several different microscopic parameters (atomic coordination number, individual atomic potential energy, local atomic pressure) and compare fluctuations in these microscopic parameters with fluctuations in related macroscopic quantities (total number of bonds in the system, total potential energy, pressure). Thus our approach reveals the relation between the collectivity of atomic motion and the crossover behavior. To the best of our knowledge, previous observations of collectivity of atomic motion, done, for instance, using four-point correlation functions [15–18], were focused on the region of the mode-coupling temperature T_c and the presence of T_A was not addressed in these works.

We performed molecular dynamics (MD) simulations on a single component system of particles interacting through a short-range pairwise potential. The changes in the local atomic structure with temperature are often described in terms of the changes in short (nearest neighbors) and intermediate (second and third nearest neighbors) order [19,20]. Here we describe the local structure in terms of the atomic bond, defined by the first minimum of the atomic pair distribution function (PDF) without implying a chemical bond. In our model the deep first minimum in the PDF ensures that the atomic bond and the local atomic coordination number, N_c , are well-defined. We find that the temperature dependence of the mean-square deviation in the total number of bonds in the system normalized to the mean-square deviations in the number of bonds of the individual atoms (coordination number) exhibits the same crossover behavior as does the energy of the inherent structure. Our results show that below the crossover temperature stronger correlations between bond breaking and bond formation develop. This may be interpreted as an indication that a tendency toward rigidification in the network of bonds begins around the potential energy landscape crossover temperature. Similar conclusions were obtained by comparing the temperature dependencies of global and local fluctuations in the potential energy and pressure. However, as shown below, the crossover behavior is more pronounced in the statistics of bonds rather than in potential energy or pressure. This illuminates the role of fluctuations in atomic connectivity in the crossover phenomenon. Our results provide further insights into the microscopic origin of the crossover phenomenon.

II. DETAILS OF MD SIMULATIONS

In our molecular dynamics (MD) simulations we used a single component system of particles interacting through the modified Johnson pair potential (see inset of Fig. 1) [21]. Further details of the potential can be found in Appendix A. This potential was designed to model the properties of a supercooled metallic (iron) liquid and glass. However, we are not interested in describing the properties of iron. Instead, we present the results with the hope that they are valid for any system of particles interacting through a pair potential, as long as the first minimum in the pair density function is well-defined. We chose a single component system despite its instability against crystallization in order to simplify the results as much as possible.

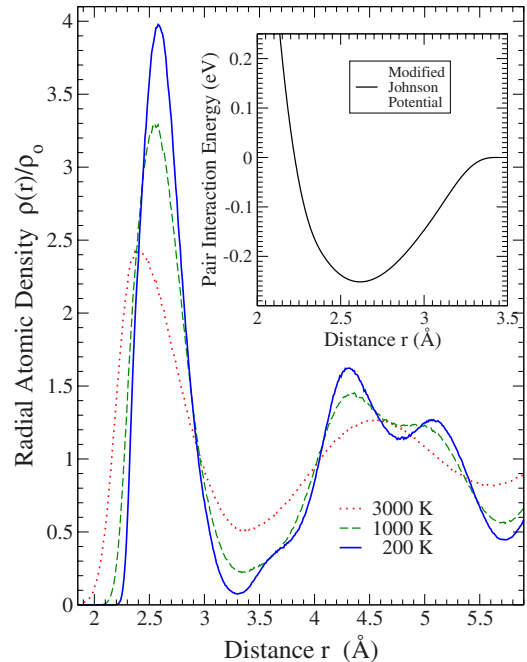


FIG. 1. (Color online) Radial pair-density function of the system at different temperatures. Note that the value of the density drops to almost zero as temperature goes to zero. Thus the first nearest neighbors are well-defined. The position of the first minimum is located at distance 3.3 Å, in the limit of zero temperature. The inset shows the modified Johnson pair potential used in our MD simulations.

The data in our MD simulations were collected at a fixed number of particles, fixed volume, and fixed energy (NVE -ensemble), with periodic boundary conditions. A fifth-order Gear algorithm was used to integrate equations of motion [22]. The simulations were performed on the systems consisting of 5488 and 1458 particles. No size effects were found for the results presented below. The initial liquid state was obtained by running MD at a high temperature (10 000 K) and at a low number density [$\rho_o=0.016$ (\AA^{-3})] starting from the *bcc* lattice. After the structure was randomized we rescaled the distances between the particles to the density of interest: $\rho_o=0.07843$ (\AA^{-3}) [23,24]. This density minimizes the energy of the *fcc* lattice with respect to the lattice spacing at $T=0$. The structures at lower temperatures were obtained by means of cooling and relaxation from this high temperature liquid state.

We controlled the temperature using a velocity rescaling algorithm [25,26] based on the formula $\langle mv_i^2/2 \rangle = 3k_B T/2$, where m is the mass of the particle, v_i is the velocity of the particle i , k_B is Boltzmann constant, and T is the temperature. During cooling and during the collection of statistics for the fluctuations in the number of bonds we applied this algorithm in two different ways. During cooling we rescaled the velocity of the particles on every MD step (the time step was chosen to be 10^{-15} s) in such a way that the average kinetic energy over all particles would correspond to the target temperature value. We found that at temperatures above 1300 K the structure of the system becomes insensitive to the history of relaxation after less than 20 000 MD steps. Thus the struc-

tures obtained by incremental cooling (with intermediate relaxations over 10^5 steps) down to 1300 K and the structures obtained by an instant drop of temperature (velocity rescaling) from 10 000 to 1300 K were indistinguishable when judged by the potential energy and the PDF.

Above 1400 K the system remained supercooled without crystallization during the simulation runs longer than 10^7 MD steps. In the temperature interval between 1300 and 700 K, crystallization into the *bcc* lattice usually occurred within $\sim 10^5$ – 10^7 MD steps depending on temperature and initial conditions. In this temperature range, slow relaxation was observed, i.e., the potential energy and the PDF were dependent on the initial conditions and the duration of relaxation. Relatively fast crystallization in this temperature range did not allow us to collect enough data for statistics of bond fluctuations. However, this temperature range is not important to the purpose of this work. Below 800 K relaxation becomes very slow. In order to avoid crystallization and obtain structures below 800 K we instantaneously rescaled the velocities of the particles from 1300 to 800 K. Further cooling was done with relaxations between the incremental temperature drops. The value of the potential energy in the system was dependent on the history of relaxation below 800 K.

When we collected the data for statistics of bond fluctuations we ran MD simulations at a constant energy in order to avoid fluctuations in the total energy affecting the bond statistics. Thus we averaged the kinetic energy over the micro-canonical ensemble and over the sampling time of 10^5 MD steps. The average value of the kinetic energy over this time interval, $\langle K(t) \rangle$, in general was slightly different from the target value K_{tar} due to a finite time step and a finite averaging time. Thus at the end of the sampling time we instantaneously rescaled the velocities of all particles, $\vec{v}_i' = \vec{v}_i \sqrt{K_{tar}/\langle K(t) \rangle}$. However, the changes in the total energy, ΔE , were very small. For example, at 2000 K we always had $\Delta E/k_B < 2$ K. Thus we essentially performed constant energy simulations.

As was observed in the previous study [27], we found that the average pressure was almost linearly dependent on temperature above 1300 K, and also below 800 K but with different slopes. Extrapolation of the data suggests that the change in the slope occurs around 800–1000 K depending on the history of cooling. This change in the slope is commonly associated with the glass transition [1,28] [see also Fig. 7(a)].

Figure 1 shows the pair density function (PDF) calculated from the structures obtained in our MD simulations at different temperatures. Note that the depth of the first minimum in the PDF approaches zero in the limit of zero temperature. Thus, as it was done in [29,30], we define an atomic bond between two particles when the distance between them is smaller than the cutoff distance corresponding to the first minimum in the pair density function, i.e., 3.3 Å.

The average atomic coordination number in our model system is around 12 to 13, as could be seen in Fig. 2. Thus the local structure in this system is in general similar to the local structure of the system composed of hard spheres [31–33], or a Lennard-Jones liquid [34–36].

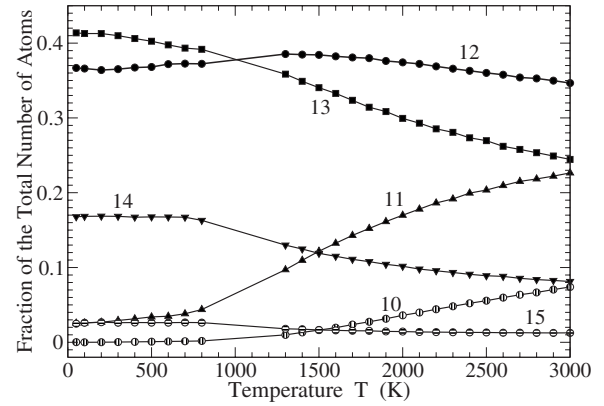


FIG. 2. Dependencies of the fractions of atoms with different coordination on temperature. The lines are guides for the eye.

III. ENERGY OF THE INHERENT STRUCTURE

The data for the inherent energy were obtained from 100 structures at each original temperature. The time separation between the two consecutive real structures was 10 000 fs at all temperatures. Each inherent structure was obtained by steepest descent relaxation of the initial structure.

The main plot in Fig. 3 shows how the average energy of the inherent structures depends on temperature. The solid circles show the energy of the inherent structure obtained from the MD simulation. The solid line is a fit using the $(1/T)$ functional form, suggested by the previous studies in the case of the Gaussian probability distribution of the potential energy minima [37–41]. The inset shows how the av-

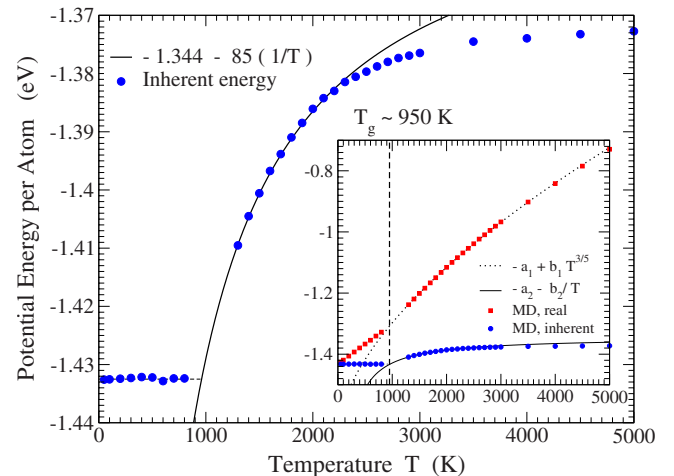


FIG. 3. (Color online) The solid circles in the main plot shows the dependence of the average inherent potential energy per atom on temperature obtained from MD simulations. The solid curve shows the fit to the data using the form and the values of parameters shown in the figure. The data below 800 K all fall on a horizontal line. Intersection of this line with the fit for the liquid state presumably gives glass transition temperature. The inset, besides the energy of the inherent structure, also shows how the energy of the “real” structure (squares) obtained from MD depends on temperature. The dotted line shows the fit to the data using the Rosenfeld-Tarazona form.

erage energies of the real (solid squares) and inherent structures (solid circles) depend on T . We see that the energy of the inherent structure is much less dependent on temperature than the energy of the real structure. This is not surprising since inherent structures do not have atomic vibrations. The purpose of the inset is to remind one that the crossover behavior is associated with rather small and subtle changes in the inherent structure. The fit (dotted line) of the dependence of the energy of the real structure on temperature was done using the Rosenfeld-Tarazona $\sim T^{3/5}$ scheme [42].

Figure 3 shows that the energy of the inherent structure deviates from the $(1/T)$ functional form above around 2300 K and becomes less strongly dependent on temperature. This defines the crossover temperature, $T_A \sim 2300$ K below which the system enters the potential energy landscape (PEL) influenced regime [2,10,43].

IV. STATISTICS OF BONDS FLUCTUATIONS

In covalent glasses such as silicate or polymer glasses the covalent bonds remain intact well above the glass transition temperature and even near the crossover temperature. In metallic glasses, however, the depth of the interatomic potential, in our case 0.25 eV (≈ 2900 K), is of the same order of magnitude as the crossover temperature. Thus atomic bonds, defined between the nearest neighbors, are dynamic: they are broken and formed with high rates all the time in the liquid state.

If bonds would form and break totally independently of each other then the mean-square deviation (MSD) in the total number of bonds, $\Sigma_{B,\text{total}}^2$ (every bond is counted once), would be essentially equal to the MSD of the local atomic coordination number, $\sigma_{B,\text{indiv}}^2$, times the number of atoms: $\Sigma_{B,\text{total}}^2 = \sigma_{B,\text{indiv}}^2 N_a / 2$, as we discuss in Appendix B. On the other hand if the bond breaking and forming are correlated these two numbers will not be equal. Thus we calculated the time average of $\Sigma_{B,\text{total}}^2(T) / N_a$ and compared it with the time and ensemble average of $\sigma_{B,\text{indiv}}^2(T)$ at different temperatures, T . In order to collect statistics we counted the total number of bonds in the system every 100 MD steps. The total length of the simulation was $\sim 10^7$ MD steps.

In Fig. 4 the open symbols show the results obtained on a system of 5488 particles, while the small closed symbols show the results obtained on a system of 1458 particles. The upper curves show the temperature dependence of the MSD in the individual particle's coordination numbers, i.e., $\sigma_{B,\text{indiv}}^2(T)$. The lower curves show the temperature dependence of the MSD in the total number of bonds (every bond is counted once) normalized to the number of atoms, i.e., $\sigma_{B,\text{total}}^2(T)$.

The temperature dependence of the ratio,

$$X(T) = \frac{\sigma_{B,\text{total}}^2(T)}{\sigma_{B,\text{indiv}}^2(T)}, \quad (1)$$

is shown in Fig. 5. The ratio $X(T)$ is nearly constant above ~ 2500 K, but it starts to decrease as temperature is reduced below, and more rapidly below 1000 K. By extrapolating the linear portions of the data we identify two crossover tem-

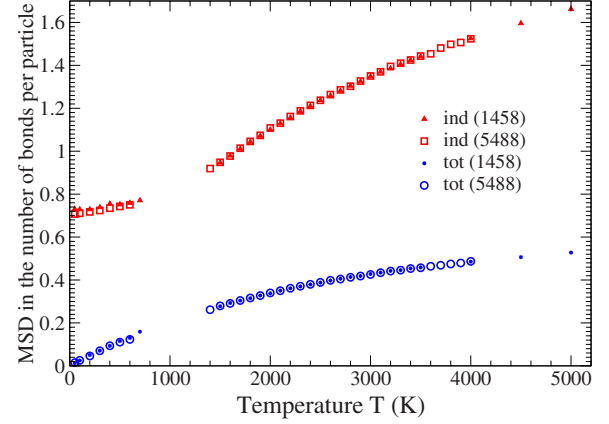


FIG. 4. (Color online) The upper curves show the temperature dependence of the MSD in the individual particle's coordination numbers, i.e., $\sigma_{B,\text{indiv}}^2(T)$. The lower curves show the temperature dependence of the MSD in the total number of bonds (every bond is counted once) normalized to the number of atoms, i.e., $\sigma_{B,\text{total}}^2(T)$. The results from the systems of 5488 and 1458 particles are shown as large open symbols and small closed symbols.

peratures, the first one close to 950 K and the second one around 2300 K. These two may be identified as the glass transition temperature, T_g , and the crossover temperature, T_A . The values of T_g and T_A are independent of the system size for $N_a = 1458$ and 5488.

The rapid decrease in $X(T)$ below 950 K must be the consequence of the system freezing into a glass. There should be two kinds of bond fluctuations: One is due to configurational rearrangements while the other is due to vibrational atomic motion. Atomic diffusion with displacements larger than interatomic distances leads to essentially irreversible changes in atomic connectivity. The fluctuations in the number of bonds due to such processes could be considered as configurational fluctuations in the network of bonds. On the other hand some of the vibrational motions of atoms around their

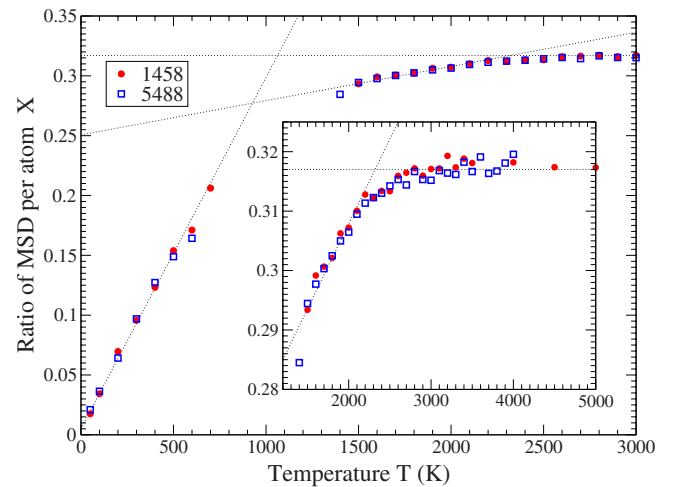


FIG. 5. (Color online) Temperature dependence of $X(T) = \sigma_{B,\text{total}}^2(T) / \sigma_{B,\text{indiv}}^2(T)$. The $X(T)$ is nearly constant above ~ 2500 K, while it decreases below. See text for discussion. Open symbols show the results from the system of 5488 particles, while closed symbols show the results from system of 1458 particles.

temporal equilibrium positions can also lead to the temporal changes in connectivity. This will happen when the interatomic distance happens to be close to the cutoff distance used to define the nearest neighbors and vibration moves the atom across the cutoff. The fluctuations in the number of bonds due to such dynamic processes could be considered as vibrational fluctuations. Below T_g the configurational fluctuations are essentially frozen, so that $\sigma_{B,\text{total}}^2(T)$ reflects only the vibrational contributions, and extrapolates to zero at $T=0$ K, as it should. On the other hand $\sigma_{B,\text{indiv}}^2(T)$, i.e., MSD of the individual particles coordination numbers, reflects the fact that different atoms can have different coordinations. Thus it is non-zero even at zero temperature as seen in Fig. 2. Therefore the ratio, $X(T)$, extrapolates to zero at $T=0$ K.

The change at T_A is more subtle. Whereas the glass transition at T_g occurs through the system falling out of equilibrium because of slow kinetics, the system has to be in equilibrium in the vicinity of T_A . In terms of the potential energy landscape (PEL) approach the decrease in the inherent energy below T_A occurs because the system spends more time in the potential energy landscape metabasins and spends less time between the metabasins, since in order to make transitions between the metabasins the system has to overcome large potential energy barriers. In the framework of the above reasoning, the decrease in the values of $X(T)$ below the crossover temperature could mean that transitions between different metabasins require larger deviations in the total number of bonds from an average value. As these transitions become more and more rare the ratio $X(T)$ starts to decrease.

A different view is that the decrease in $X(T)$ means that the network of bonds becomes more rigid below the crossover temperature as discussed below. The stronger tendency to conserve the total number of bonds, of which $X(T)$ is a representative, is a signature of this behavior. Thus the decrease in $X(T)$ could essentially signify the beginning of the transition from a liquid to a glass.

V. FLUCTUATIONS IN POTENTIAL ENERGY AND PRESSURE

Similar to the fluctuations in the number bonds, we can also consider fluctuations in the total potential energy vs fluctuations in the potential energy of individual atoms, since the potential energy and the number of bonds are related quantities. As we described previously, we ran essentially constant total energy simulations. However, while the total energy is fixed the values of the potential and kinetic energies fluctuate with time. In order to estimate the mean-square deviation (MSD) of the total potential energy we ran simulations for $\sim 10^7$ MD steps and we evaluated the value of the total potential energy, $\sigma_{U,\text{total}}^2$, as well as the MSD in the potential energy of the individual atoms, $\sigma_{U,\text{indiv}}^2$, every 20 MD steps. The summary of the obtained data is presented in Fig. 6. The plot (c) of this figure shows the ratio, $Y(T) = \sigma_{U,\text{total}}^2 / \sigma_{U,\text{indiv}}^2$. The results again suggest the existence of a gradual crossover behavior around the temperature between 2000 and 3000 K.

However, the comparison between the inset of Figs. 5 and 6(c) shows that crossover is much more pronounced if ex-

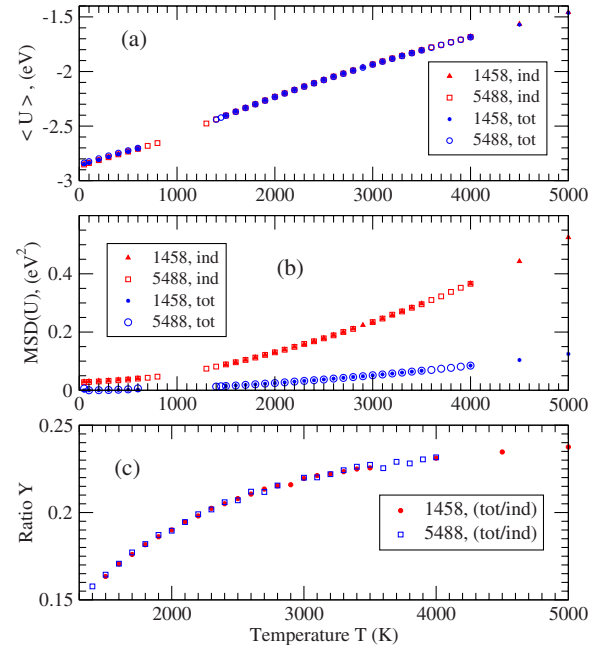


FIG. 6. (Color online) (a) The temperature dependence of the average value of the potential energy of the system. (b) The MSD of the total potential energy per atom $\sigma_{U,\text{total}}^2$ (lower curves) and the MSD of the individual particle's potential energy $\sigma_{U,\text{indiv}}^2$. (c) The temperature dependence of the ratio $Y(T) = \sigma_{U,\text{total}}^2 / \sigma_{U,\text{indiv}}^2$.

pressed in terms of simple connectivity units (bonds) as in Fig. 5. We find it quite remarkable that simple geometrical features show the crossover more clearly than does the potential energy. The possible reason for this could be that most of the atomic vibrations other than those of the pairs of atoms close to the cutoff distance do not contribute to bond fluctuations, whereas the potential energy reflects all the vibrations. This is similar to the situation for the inherent structure where atomic vibrations are removed by steepest descent relaxation, and the temperature dependence in the topology of atomic connectivity is revealed.

We have also compared the fluctuations in the global pressure and those in the local pressure on the individual particles. The total pressure in the system for a particular configuration of the particles could be calculated according to

$$P = -\frac{1}{3V} \sum_{ij} \left[r_{ij} \left(\frac{\partial \phi}{\partial r_{ij}} \right) \right]. \quad (2)$$

The local, or atomic-level, pressure was defined earlier [24]. The atomic-level pressure on an atom i can be calculated as

$$p_i = -\frac{1}{6V_i} \sum_j \left[r_{ij} \left(\frac{\partial \phi}{\partial r_{ij}} \right) \right], \quad (3)$$

where the sum over j covers the neighbors within the range of the potential, 3.44 Å. The local atomic volume of an atom i could be calculated as

$$V_i = \frac{4}{3} \pi r_i^3, \quad (4)$$

where

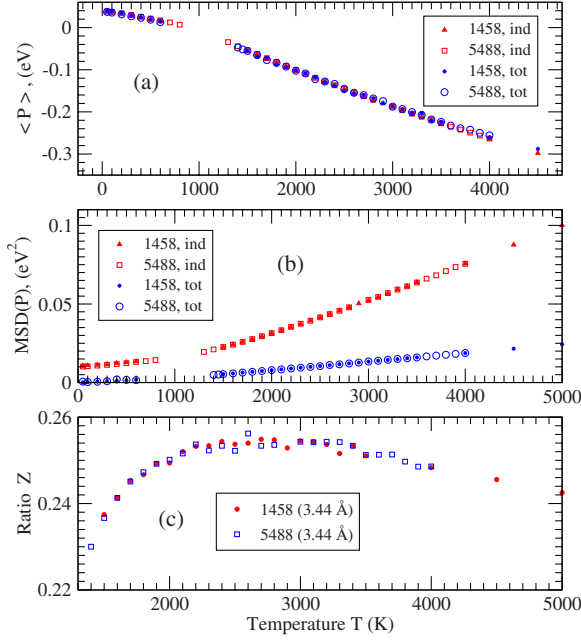


FIG. 7. (Color online) (a) The temperature dependence of the average value of the pressure. (b) The MSD of the total pressure (2) per atom, $\sigma_{P,\text{total}}^2$ (lower curves) and the MSD of the pressure (3) of the individual particles $\sigma_{P,\text{indiv}}^2$ (upper curve). (c) The temperature dependence of the ratio $Z(T) = \sigma_{P,\text{total}}^2 / \sigma_{P,\text{indiv}}^2$.

$$r_i = \left(\sum_j w_{ij} r_{ij} \right) / \left(\sum_j w_{ij} \right), \quad w_{ij} = (1/r_{ij}^2). \quad (5)$$

The sums in Eqs. (4) and (5) are again over the nearest neighbors. The weighing factor w_{ij} is proportional to the solid angle that atom j blocks as seen from an atom i .

Figure 7(a) shows how average pressure depends on temperature. This plot suggests that there is a glass transition around 1000 K. Figure 7(b) presents the temperature dependence of the MSD of the global pressure per atom, $\sigma_{P,\text{total}}^2$ and the MSD of the atomic-level pressure $\sigma_{P,\text{indiv}}^2$. The temperature dependence of the ratio $Z(T) = \sigma_{P,\text{total}}^2 / \sigma_{P,\text{indiv}}^2$ is shown in Fig. 7(c).

The results suggest that atomic pressures on different sites do not fluctuate independently and that correlations in pressure fluctuations on different sites exhibit nontrivial temperature dependence. Thus if the local pressure on a certain atom increases because of some structural change, then at low temperatures it becomes more and more probable that the local atomic pressure on some other atom will decrease. Thus the correlated changes in the local pressure on different atoms tend to keep the total average pressure constant, and thus these correlations decrease the MSD in total pressure compared to the MSD in the local atomic pressures. As it was shown in [44], the local atomic-level pressure is related to the coordination number. When the coordination number is smaller than the average then, on average, the central atom is under compression. On the other hand if it is larger than the average then the central atom feels the expansive (negative) pressure. Thus the similarity in the results in Figs. 5 and 7 is not an accident.

VI. DISCUSSION

The major result of this paper is that we have found evidence that the crossover behavior previously observed in the inherent structure could also be seen in the dynamics of the real structure. This conclusion is derived from the comparison of fluctuations (mean-square deviations) in the global properties vs fluctuations in the local properties. In particular we considered fluctuations in the number of bonds (i.e., fluctuations in the atom network connectivity) as well as fluctuations in the potential energy and pressure. All the results consistently demonstrate that they all contain the evidence of crossover phenomenon at the same temperature, which is also the crossover temperature observed in the inherent structure.

There are several previous observations of crossover behavior on real structures which include temperature dependence of β in stretched exponential fit to the intermediate self-scattering function [10,13], temperature dependence of viscosity and breakdown of the Stokes-Einstein relationship [13,14], and deviation from the fluctuation-dissipation relation [13].

The present results add to these observations and bring some insights into the nature and origin of the crossover phenomenon. In this work the crossover behavior was most clearly observed in the temperature dependence of the ratio between the mean-square deviations in the total number of bonds and the mean square deviation in the coordination number of individual atoms, $X(t) = \sigma_{B,\text{total}}^2 / \sigma_{B,\text{indiv}}^2$. $X(T)$ exhibits a marked change around $T_A \sim 2300$ K, well above the glass transition temperature. This temperature coincides with the temperature at which the energy of the inherent structure starts to deviate from the expected $1/T$ temperature dependence (i.e., the crossover temperature) which is also around ~ 2300 K. Thus the way in which the system samples the potential energy landscape is reflected in the correlations between the bond breaking and bond forming. A similar crossover was also observed in the ratio between the mean-square deviations in the global pressure and the mean-square deviation in the atomic-level pressure, $Z(T) = \sigma_{P,\text{total}}^2 / \sigma_{P,\text{indiv}}^2$.

When an atomic bond between the atoms i and j is cut, the coordination number is reduced by one at both atoms, whereas when a bond is created the coordination number is increased by one for the two atoms involved. Since the local coordination number is linearly related to the atomic-level pressure [44], the fluctuations in bonds must be related to the fluctuations in the atomic level pressure. Indeed the similarity in the behaviors of $X(T)$ and $Z(T)$ underscores this point. Again, as we discussed on the relation between $X(T)$ and $Y(T)$ this correspondence is not perfect, since $Y(T)$ and $Z(T)$ include contributions from all the atomic vibrations, while only small portions of the atomic vibrations affect $X(T)$.

It was shown previously that spatial correlations develop in the local atomic shear stresses, even above the glass transition temperature, in the system studied in this work [27]. Strong correlations are seen between the nearest neighbors that decrease with distance. The onset of correlations is around 2000 K or higher. In our view this observation is directly relevant to our results. At high temperatures local shear stresses fluctuate freely without correlation, but as tem-

perature is lowered they start to interact with each other.

It is natural to assume that the local stresses interact with each other through the dynamic stress fields, including the phonon fields. Although liquids do not support static stress fields, they could support dynamic stress fields. They certainly support dynamic pressure fields, since the bulk modulus of a liquid is not much different from that of a solid, and sound waves propagate in the liquid. On the other hand it may appear less likely that the shear stress fields are supported by the liquid, since the shear modulus is zero. However, the shear modulus is frequency-dependent, and at high enough frequency and low enough temperature dynamic shear fields may be present in the liquid. The correlations reported in Ref. [27] are the evidence of the existence of such fields. The observed correlations are instantaneous (same time), but dynamic correlations that decay with time must be present as well in the liquids, in a similar temperature range. We are currently examining such local dynamic shear stress correlations in relation to the Green-Kubo expression for viscosity.

In the glassy state such correlations can be modeled [44,47] by the continuum mechanics theory of Eshelby [46]. According to the Eshelby theory pressure centers interact with each other through the shear fields. Thus the local pressure fluctuations, and therefore bond fluctuations, become correlated only when the dynamic shear stress fields are present. Then the onset of such dynamic shear stress fields could cause the crossover phenomenon. The closeness of the onset temperature for shear stress correlation to the crossover temperatures that characterize the changes in $X(T)$, $Y(T)$, and $Z(T)$ strongly supports this possibility.

If the onset of the dynamic shear stress fields is the origin of the crossover phenomenon, it leads to an interesting possibility that the metabasin in the energy landscape may be defined by the communication through such dynamic shear stress fields. At high temperatures local topology defined by bonds fluctuates almost freely, so that the system does not see the energy landscape. The properties are determined mostly by local energy fluctuations. Below the crossover temperature, however, local fluctuations start to communicate through the dynamic shear stress fields, so the local fluctuations are no longer independent, and start to develop the energy landscape. It is therefore likely that the features of the energy landscape will be made clearer by studying the detailed aspects of the local dynamic stress correlations. This subject will be discussed in our future publications.

VII. CONCLUSION

The results discussed in this paper indicate that the crossover phenomenon is characterized by the increase in the correlations between bond breaking and forming as well as the onset of interaction among the local pressure fluctuations. Since the bond breaking and forming change the atomic level pressure, these two observations describe essentially the same phenomenon. According to the continuum theory of mechanics [46], pressure centers interact with each other through the shear stress fields. Together with the earlier observation [27] on the development of spatial correlations in

instantaneous local shear stresses, this result suggests an interesting possibility that the crossover phenomenon is caused by the onset of dynamic shear stress fields. The crossover phenomenon could be considered as a signature of the liquid becoming more rigid and assuming a more solidlike character.

ACKNOWLEDGMENTS

This research has been sponsored by the Division of Materials Sciences and Engineering, Office of Basic Energy Sciences, U.S. Department of Energy under Contract No. DE-AC05-00OR-22725 with UT-Battelle, LLC. We would like to thank J. C. Phillips, M. F. Thorpe, Y. Y. Braiman, B. V. Fine, and K. A. Lokshin for useful discussions.

APPENDIX A: MODIFIED JOHNSON PAIR POTENTIAL

The form of the modified Johnson pair potential used in this study is slightly different from the one that was used previously [45]. The minimum allowed distance used in the previous form was 1.9 Å, while we found that at temperatures above 3000 K atoms can come closer than 1.9 Å. Thus we had to modify potential at small distances. In our present work we used the potential which coincides with the form described previously [45] at distances larger than 2.4 Å. For the distances smaller than 2.4 Å the form of the potential was slightly modified. The full form of the potential is given below (the intervals of distance r are in Å and pair potential energy is in eV).

For [$0 < r \leq 2.246\ 948$] the potential has the form

$$\begin{aligned} \phi(r) = & 2.463\ 595(r - 2.977\ 441)^4 \\ & - 1.396\ 616(r - 2.977\ 441)^2. \end{aligned}$$

For [$2.246\ 948 < r \leq 2.4$] the potential has the form

$$\begin{aligned} \phi(r) = & -12.900\ 210(r - 2.4)^4 - 15.096\ 180(r - 2.4)^3 \\ & + 1.372\ 738(r - 2.4)^2 - 0.504\ 775(r - 2.4) \\ & - 0.200\ 211. \end{aligned}$$

For [$2.4 < r \leq 3.0$] the potential has the form

$$\begin{aligned} \phi(r) = & -0.639\ 230(r - 3.115\ 829)^3 \\ & + 0.477\ 871(r - 3.115\ 829) - 0.092\ 606. \end{aligned}$$

For [$3.0 < r \leq 3.44$] the potential has the form

$$\begin{aligned} \phi(r) = & 14.671\ 110(r - 3.0)^5 - 12.910\ 630(r - 3.0)^4 \\ & + 1.725\ 326(r - 3.0)^3 + 0.222\ 124(r - 3.0)^2 \\ & + 0.452\ 143(r - 3.0) - 0.146\ 964. \end{aligned}$$

The potential defined in this way has a continuous second derivative everywhere.

APPENDIX B: PROBLEM OF BOND COUNTING

Here we estimate the value of the ratio of the MSD in the total number of bonds (normalized to the number of atoms)

to the MSD in the number of bonds for uncorrelated atoms for a very simple model.

Let us suppose that we have a lattice. We assume that the coordination number of every atom is N_c^a . We also assume that every bond in the lattice fluctuates in such a way that the average ratio of the length of time t_1 when it exists to the length of time t_2 when it does not exist is t_1/t_2 . Let us also assume that all bonds fluctuate independently.

Under the assumptions above the contribution of one bond to the average number of bonds of an individual atom is given by

$$\bar{n}_{1b} = \frac{1}{(t_1 + t_2)} \int_0^{t_1} dt = \frac{t_1}{(t_1 + t_2)}, \quad (\text{B1})$$

while the MSD from the average value (for one bond) is given by

$$\begin{aligned} \sigma_{1b}^2 &= \frac{1}{(t_1 + t_2)} \left[\int_0^{t_1} (1 - \bar{N}_{1b})^2 dt + \int_0^{t_2} (0 - \bar{N}_{1b})^2 dt \right] \\ &= \frac{t_1 t_2}{(t_1 + t_2)^2}. \end{aligned} \quad (\text{B2})$$

Since all bonds fluctuate independently the average number of bonds and mean-square deviation in the number of bonds for one atom are

$$\bar{N}_{1a} = N_c^a \bar{n}_{1b}, \quad \sigma_{1a}^2 = N_c^a \sigma_{1b}^2. \quad (\text{B3})$$

Let us now consider the whole lattice. The contributions of every bond to the total number of bonds in the lattice and to the mean-square deviation are still given by Eqs. (B1) and (B2). Thus the total average number of bonds in the whole lattice and the mean-square deviation are given by

$$\bar{N}_L = \left(\frac{N_a N_c^a}{2} \right) \bar{n}_{1b}, \quad \sigma_L^2 = \left(\frac{N_a N_c^a}{2} \right) \sigma_{1b}^2, \quad (\text{B4})$$

where $(N_a N_c^a / 2)$ is the total number of bonds in the lattice (if every bond is counted once as in Fig. 4).

Thus we conclude that the ratio of the MSD in the total number of bonds per atom to the msd in the number of bonds for one atom is

$$\frac{1}{N_a} \frac{\sigma_L^2}{\sigma_{1a}^2} = \frac{1}{2}. \quad (\text{B5})$$

Thus this model suggests that because of the way the bonds are counted the value of the ratio of the MSD in the total number of bonds (normalized to the number of atoms) to the MSD in the number of bonds for one atom should be 1/2. The fact that the value of the ratio calculated in MD simulations is smaller than 1/2 indicates that there are correlations in bond breaking and formation.

-
- [1] P. G. Debenedetti, *Metastable Liquids: Concepts and Principles* (Princeton University Press, Princeton, NJ, 1996).
- [2] P. G. Debenedetti and F. H. Stillinger, *Nature (London)* **410**, 259 (2001).
- [3] W. Kauzmann, *Chem. Rev. (Washington, D.C.)* **43**, 219 (1948).
- [4] W. Zachariasen, *J. Am. Chem. Soc.* **54**, 3841 (1932).
- [5] J. C. Phillips, *J. Non-Cryst. Solids* **18**, 33 (1975).
- [6] M. H. Cohen and D. Turnbull, *J. Chem. Phys.* **31**, 1164 (1959).
- [7] G. Adam and J. H. Gibbs, *J. Chem. Phys.* **43**, 139 (1965).
- [8] C. Donati, J. F. Douglas, W. Kob, S. J. Plimpton, P. H. Poole, and S. C. Glotzer, *Phys. Rev. Lett.* **80**, 2338 (1998).
- [9] B. Doliwa and A. Heuer, *J. Non-Cryst. Solids* **307**, 32 (2002).
- [10] S. Sastry, P. G. Debenedetti, and F. H. Stillinger, *Nature (London)* **393**, 554 (1998).
- [11] T. S. Schröder, S. Sastry, J. C. Dyre, and S. C. Glotzer, *J. Chem. Phys.* **112**, 9834 (2000).
- [12] S. P. Das, *Rev. Mod. Phys.* **76**, 785 (2004).
- [13] L. Angelani, G. Parisi, G. Ruocco, and G. Vilianni, *Phys. Rev. Lett.* **81**, 4648 (1998).
- [14] P. Bordat, F. Affouard, M. Descamps, and F. Müller-Plathe, *J. Phys.: Condens. Matter* **15**, 5397 (2003).
- [15] S. C. Glotzer, V. N. Novikov, and T. B. Schröder, *J. Chem. Phys.* **112**, 509 (2000).
- [16] N. Lačević, F. W. Starr, T. B. Schröder, and S. C. Glotzer, *J. Chem. Phys.* **119**, 7372 (2003).
- [17] L. Berthier *et al.*, *Science* **310**, 1797 (2005).
- [18] L. Berthier *et al.*, *J. Chem. Phys.* **126**, 184503 (2007).
- [19] F. Yonezawa, *Glass Transition and Relaxation in Disordered Structures*, edited by H. Ehrenreich and D. Turnbull, in *Solid State Physics*, Vol. 45 (Academic, New York, 1991), pp. 179–254.
- [20] G. S. Cargill III, *Structure of Metallic Alloy Glasses*, edited by F. Seitz and D. Turnbull, in *Solid State Physics*, Vol. 30 (Academic, New York, 1975), pp. 227–320.
- [21] R. A. Johnson, *Phys. Rev.* **134**, A1329 (1964).
- [22] M. P. Allen and D. J. Tildesley, *Computer Simulation of Liquids* (Clarendon Press, Oxford, 1987).
- [23] K. Maeda and S. Takeuchi, *J. Phys. F: Met. Phys.* **8**, 3823 (1978).
- [24] T. Egami, K. Maeda, and V. Vitek, *Philos. Mag. A* **41**, 883 (1980).
- [25] L. V. Woodcock, *Chem. Phys. Lett.* **10**, 257 (1971).
- [26] D. M. Heyes, *The Liquid State: Applications of Molecular Simulations*, Wiley Tutorial Series in Theoretical Chemistry (Wiley, New York, 1998).
- [27] S.-P. Chen, T. Egami, and V. Vitek, *Phys. Rev. B* **37**, 2440 (1988).
- [28] F. Faupel, W. Frank, M. P. Macht, H. Mehrer, V. Naundorf, K. Ratzke, H. R. Schober, S. K. Sharma, and H. Teichler, *Rev. Mod. Phys.* **75**, 237 (2003).
- [29] J. D. Honeycutt and H. C. Andersen, *J. Phys. Chem.* **91**, 4950 (1987).
- [30] R. Yamamoto and A. Onuki, *Phys. Rev. E* **58**, 3515 (1998).
- [31] J. D. Bernal, *Nature (London)* **188**, 910 (1960).
- [32] G. S. Cargill, *J. Appl. Phys.* **41**, 2248 (1970).
- [33] J. L. Finney, *Proc. R. Soc. London, Ser. A* **319**, 479 (1970).

- [34] L. Verlet, Phys. Rev. **159**, 98 (1967).
[35] L. Verlet, Phys. Rev. **165**, 201 (1968).
[36] J. L. Finney, Proc. R. Soc. London, Ser. A **319**, 495 (1970).
[37] A. Heuer, Phys. Rev. Lett. **78**, 4051 (1997).
[38] S. Büchner and A. Heuer, Phys. Rev. E **60**, 6507 (1999).
[39] S. Mossa, E. La Nave, H. E. Stanley, C. Donati, F. Sciortino, and P. Tartaglia., Phys. Rev. E **65**, 041205 (2002).
[40] S. Sastry, Nature (London) **409**, 164 (2001).
[41] Y. Gebremichael, M. Vogel, M. N. J. Bergroth, F. W. Starr, and S. C. Glotzer, J. Phys. Chem. B **109**, 15068 (2005).
[42] Y. Rosenfeld and P. Tarazona, Mol. Phys. **95**, 141 (1998).
[43] M. Goldstein, J. Chem. Phys. **51**, 3728 (1969).
[44] T. Egami and D. Srolovitz, J. Phys. F: Met. Phys. **12**, 2141 (1982).
[45] T. Tomida and T. Egami, Phys. Rev. B **52**, 3290 (1995).
[46] J. D. Eshelby, Proc. R. Soc. London, Ser. A **241**, 376 (1957).
[47] D. Srolovitz, T. Egami, and V. Vitek, Phys. Rev. B **24**, 6936 (1981).